Multispectral Imaging with a Modified DSLR Camera

Tiper Korneles Muwarberto Uniplaita, Donny Danudirdjo, and Andriyan Bayu Suksmono
School of Electrical Engineering and Informatics, Bandung Institute of Technology, Bandung, Indonesia
t.uniplaita@yahoo.com

***Abstract*—This paper describes a multispectral imaging system using a Canon EOS 1000D camera, photographic lenses, and a dispersive element. The system consists of three subsystems: a PVC holder to arrange the optical devices that can be connected to the camera, an acrylic frame to support the position of the PVC holder, and expectation maximization algorithm to reconstruct the spectral-spatial data cube. We perform a calibration process to output the reference matrix of the reconstruction using four LEDs with different wavelengths. The output of the system is a data cube in the form of 20 images that represent the observed intensity response from 455 nm to 645 nm.**

Keywords—multispectral imaging; spectral image reconstruction; spectrum measurement

I. Introduction

Spectral imaging is a method to measure electromagnetic spectrum at object surface. For the past two decades, the output of spectral imaging has been used to identify matters that compose an object. A science team used spectral data from a satellite that carries a spectral imaging system to map a mineral site at Mount Fitton in South Australia [1]. Joseph et al [2] combine a hyperspectral optical imager and an image analysis technique such as support vector machine to diagnose breast cancer, cervical cancer, and melanoma cancer in human tissue. Spectral imaging systems can also be used to investigate evidence in crime scenes. Crane et al [3] non-invasively detect latent fingerprints on a postcard, a garbage bag, and a US dollar bill used a infrared spectroscopy imager. In the food industry, to improve product quality, Wu et al [4] use a hyperspectral imager to determine water distribution within beef during dehydration process.

Although spectral imaging technology offers a great benefit over conventional imaging system, its application was initially limited for aerial observations [5]. Recently, there are proposals for generic spectral imaging systems such as the ones in [6–8]. These systems are usually developed using a Charge-Couple Device (CCD) sensor, a diffraction grating, and a light filter. More recently, Habel [9] made a spectral imaging system using a Canon EOS Mark II camera and optical devices for photography.

This paper describes the development of a multispectral imaging system using a Canon EOS 1000D camera, a set of photographic lenses and a dispersive element made by a compact disc (CD). We follow the optical configuration in [9] to obtain similar measurement range. The differences are in the image sensors used and the focal-lengths of the lenses.

II. Theory

The output of spectral imaging is a three-dimensional data cube which consists of spatial and spectral coordinates as shown in Fig. 1 [6].

A. Spectral imaging methods

In general, there are three methods to obtain a data cube: spatial scanning method, spectral scanning method, and non-scanning method.

Systems that use spatial scanning method obtain all spectral data from a part of the object at one image acquisition. The same process is then repeated for other parts of the object until all voxels of the data cube are collected. Hoye et al [6] develop a hyperspectral imager using an optical relay and a diffraction grating. The diffraction grating is used as the dispersive element to obtain all spectral data of a part of the object. The optical relay is used to set the part that is projected onto the diffraction grating.

Systems that use spectral scanning method obtain spectral data from all spatial areas for each wavelength. In [7], Brauers et al combine a filter wheel and a rotary machine for their multispectral imager. The rotary machine is used to adjust the position between the filter wheel and a monochrome camera. Hardeberg et al [8] use a Liquid Crystal Tunable Filter (LCTF) as the dispersive element to obtain the data cube. They control bandwidth of the crystal by changing its voltage level.

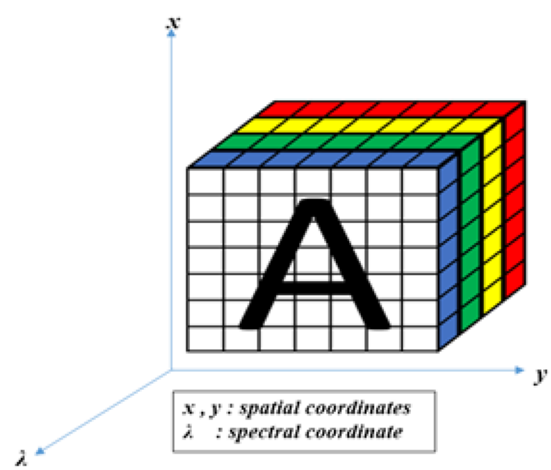

Fig. 1. Model of a data cube

Systems that use non-scanning method only need one image acquisition to obtain full spectral and spatial data of the cube. The non-scanning eliminates the use of mechanical devices and light filters. Habel et al [9] develop a practical spectral imager using Computed Tomography Imaging Spectroscopy (CTIS) that is a form of the non-scanning.

B. Principle of CTIS

The main component of CTIS is the diffraction grating which projects a beam with a projection angle that is comparable with its wavelength to the sensor [10]. As shown in Fig. 2, if plane-A that is composed of many wavelengths passes through the diffraction grating then it will be projected to plane-B at different angle.

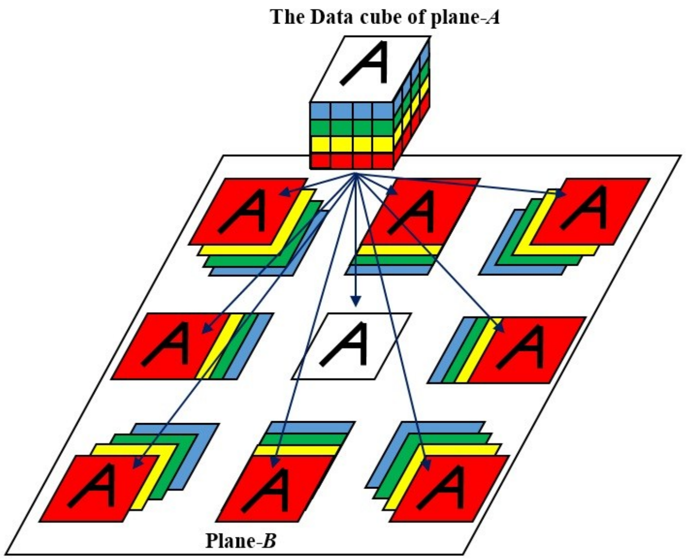

Fig. 2. Projection of plane-A to plane-B through a cross diffraction grating.

Fig. 2 shows a projection model of a cross diffraction grating. Plane-*A* is projected in two modes: zero mode and first-order mode. Zero mode is the projection of plane-*A* in the middle of plane-*B*, and first-order mode is the projection around the zero mode. The relation between the cube which passes through a diffraction grating and its projection on plane-B can be described by a linear equation

$$g = H.f \quad (1)$$

where *f* is the data cube on plane-*A*, *g* is the projection of the data cube on plane-B and *H* is the transform matrix that represent the characteristic of the diffraction grating. The projection *g* contains spectral and spatial information from *f*. As shown in Fig. 2, however, these two information overlap. One way to reconstruct the spatial and spectral information from *g*, among others, is the EM algorithm

$$\hat{f}_n^{k+1} = \frac{\hat{f}_n^k}{\sum_{m=1}^{M} H_{mn}} \sum_{m=1}^{M} H_{mn}^T \frac{g_m}{H\hat{f}^k{}_m} \quad (2)$$

which uses *f*, g, and *H* in the form of matrix.

In this system, plane-B is the camera sensor. The sensor records projection of an object in the form of raw image. The intensity of each pixel in the raw image is stored in *g*, which is produced every time an object is captured by the camera.

A calibration needed to fill *H* is described in Section 4. The obtained H is then used to reconstruct *g* using (2). The result of reconstruction process is a data cube that is stored in *f*. The same *H* can also be used to reconstruct *g* from different objects as long as the optical configuration of the system does not change.

III. SYSTEM DESIGN

The implemented multispectral imaging system is divided into three subsystems: a modified camera to perform the data acquisition, a calibration equipment to fill the reconstruction matrix *H*, and a implementation of the reconstruction algorithm to obtain the data cube.

There are three factors behind the camera modification. First, the camera system uses an optical configuration similar to [9] in order to obtain the same measurement range, as shown in Fig. 3. Second, we use a camera with a good HDR (high dynamic range). A camera with a good HDR has a wide range intensity level that is helpful to compensate the decrease of light intensity after passing through a diffraction grating. Third, the system uses a CD (compact disk) element as the diffraction grating. Two CDs are put on a similar position, the first CD is rotated 90 degrees toward the other CD to form a cross grating pattern as shown in Fig. 4.

Based on the three conditions before, we use Canon EOS 1000D camera with 14-bit HDR and two CD elements with 625 lines/mm diffraction index [10] as the diffraction grating. For the other lenses, we follow the same specification used in [9].

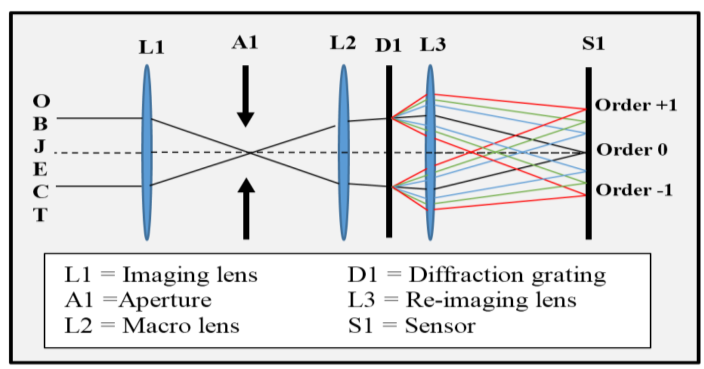

Fig. 3. The optical configuration used in the system

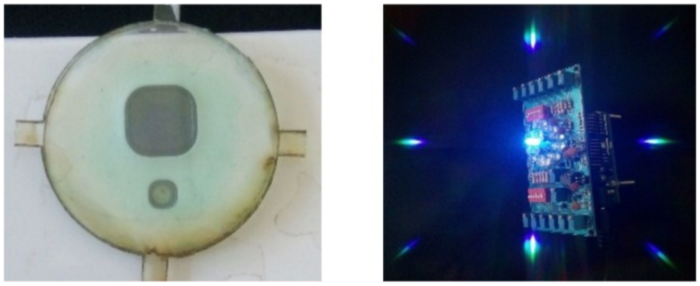

(a) (b)

Fig. 4. (a) Two CDs are placed in front of a mobile phone camera (b) Image of 465 nm LED taken by the mobile phone camera–CD configuration in (a).

Fig. 5 shows parts of the modified camera. First, a 2 inches female PVC adapter as a 50 mm lens holder. Second, a 2 inches male PVC adapter as a square aperture holder. Third, a 3 inches PVC couple as a buffer of the 50 mm lens and the square aperture to an 18 mm camera lens. Fourth, a camera that is connected to the 18 mm lens. A 100 mm concave lens as collimating lens and two CDs are mounted in front of the 18 mm lens.

The EM reconstruction algorithm is implemented on Matlab 2013a. We adjust the size of H, as well as that of g and f, so that the reconstruction program can run on a computer with 2 GB of RAM. The size of canon EOS 1000D's raw image is 2602×3906 pixels. In order to reduce the size of g, the reconstruction program down-samples the raw image to the size of 261×391 pixels, and then the elements of g are obtained from specified areas of the raw image as shown in Fig. 7. The red squares in Fig. 7 are the border of projection area of the first-order mode, and the white square is the border of a projection area of a zero mode. The size of zero mode area in down-sampled image is 20×20 pixels, determined by the optical configuration of the system and the size of the square aperture. The size of every first-order mode area in down-sampled image is 20×56 pixels, determined by the size of zero mode area in the down-sampled image and the pixel distance between the projection of 465 nm and 635 nm LEDs in the first-order mode area of the down-sampled image. The 465nm and 635 nm LEDs are the lowest and highest LED wavelength that are used in the calibration process. All pixels in first-order mode and zero mode projection areas are put in a matrix with the size of 5040×1.

The matrix f contains information about intensity of an object in all measurement bands. Each band contains 400 intensity values of 20×20 pixels in zero mode area of the down-sampled image. The number of band that is designed in this system is 20, hence the size of f becomes 8000×1. It is based on the number of total pixel in the zero mode area, and the number of this system's band. Based on the size of g and f, the size of H to 5040×8000.

IV. Calibration

Fig. 6 shows the components used for calibration. First, a camera holder that is designed to hold the camera and the PVC pipes in the same position during the calibration process. The structure of the camera holder is made based on the shape of the PVC pipes. Second, a spatial point plane that has tiny holes as spatial information during the calibration process. Third, an LED board that provides spectral information during the calibration process. Each LED is placed in a small hole in the spatial point plane and its image is then captured by the camera.

The calculation of the distance between the 50mm lens and the spatial point plane follows two equations

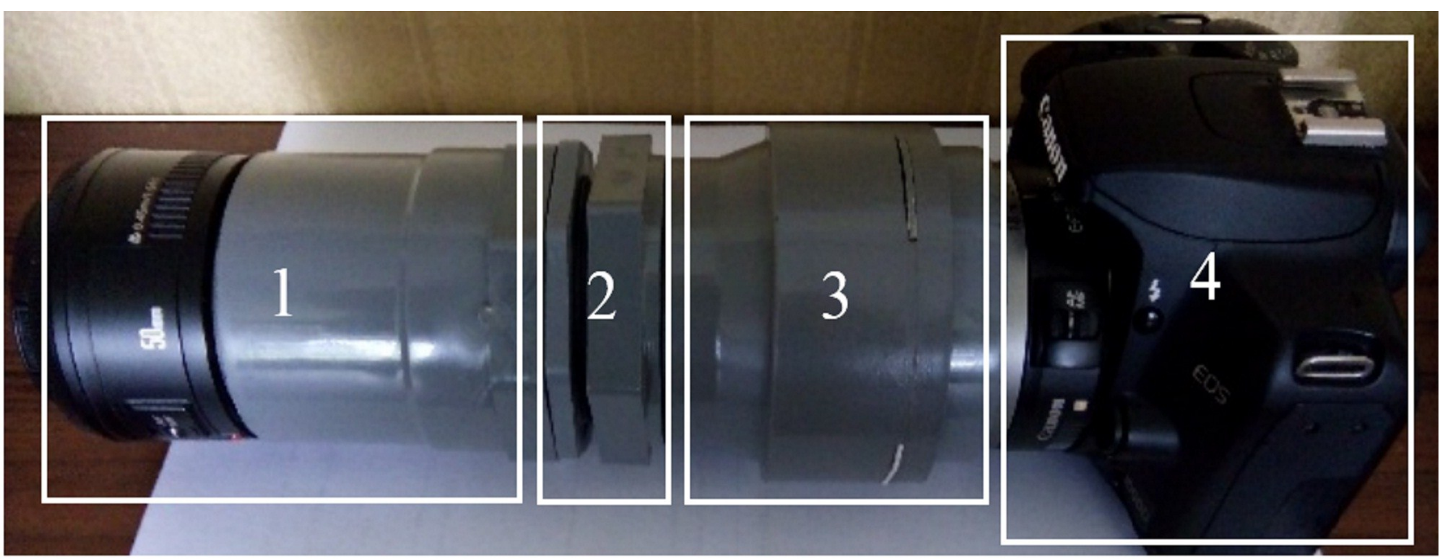

Fig. 5. The construction of a modified camera

$$\frac{1}{f} = \frac{1}{s} + \frac{1}{s'} \quad (3)$$

$$\frac{h'}{h} = \frac{s'}{s} \quad (4)$$

where f is a focal length of the 50 mm lens, s is the distance between an object and the 50 mm lens, s' is the distance between the 50 mm lens and the formed shadow, h is the size of the object, and h' is the size of the shadow. The distance between the spatial point plane and the 50 mm lens is 67.5 cm based on (3) and (4). At that distance, the system is capable to capture an image of the spatial point plane with size of 6.25×6.25 cm^2. The distance between the 50 mm lens to the square aperture is set at 54 mm. To fill H, the system needs two kinds of information. First, projected voxels of the data cube into the sensor plane of the camera. Second, a camera spectral response throughout the measurement range.

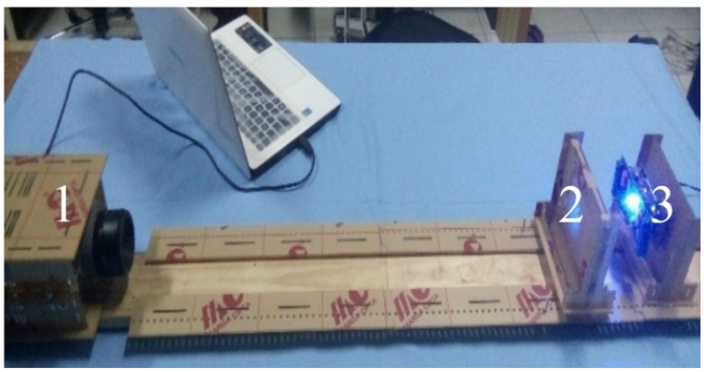

Fig. 6. Arrangement of the components for system calibration.

A. Projection of the data cube to the sensor plane

The information about voxels projection of the data cube to the sensor plane is obtained from image acquisitions of 465 nm, 525 nm, 590 nm and 635 nm LEDs. Each LED is captured by the camera at different positions in the zero mode of the down-sampled image as shown in Fig. 7. The spatial position of an LED in the zero mode represents the spatial coordinate of a voxel in the data cube. Whereas, the wavelength of an LED represents the spectral coordinate of a voxel in the data cube. Each LED with different wavelength has different spatial positions.

The distance between the zero mode and the first-order modes of all LEDs is calculated and averaged over all of the spatial positions in the zero mode. Whereas, the distance between the zero mode and the first-order modes for another projection voxels in the measurement range is obtained from interpolation and extrapolation of these four wavelengths. The information is used to find out the projection of each voxel in the data cube to the area of first-order modes in the down-sampled image.

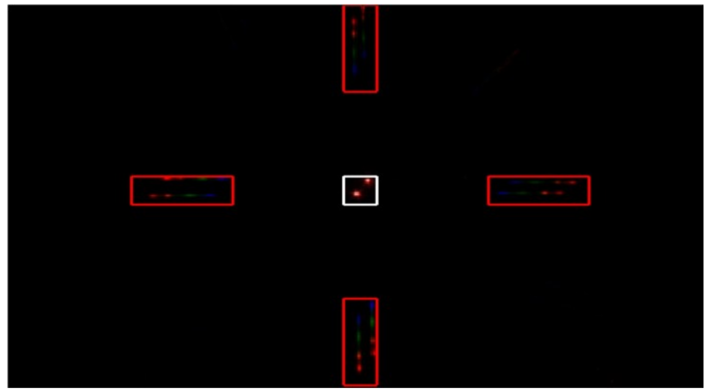

Fig. 7. A down-sampled image of 465 nm, 525 nm, 590 nm, and 635 nm LED projection.

B. The Spectral Response of Canon EOS 1000D Camera

The values of the camera spectral response are used to adjust the intensity level of the down-sampled image while the reconstruction process. The calculation of the camera spectral response is done using 465 nm, 525 nm, 590 nm, and 635 nm LEDs. The intensity of LEDs is measured using a PDA100A sensor with a known spectral response [11]. The LED intensity is calculated according to

$$\text{LED intensity} = \frac{\text{PDA100A output}}{\text{PDA100A responsivity}}. \quad (5)$$

Each calibrated LED is captured using the compact camera so that there are four images of calibrated LEDs. The values of camera spectral response are obtained by dividing the intensity of each LED projection with the real intensity of each LED calculated using (5). The camera spectral response for other wavelengths is calculated using polynomial interpolation. Fig. 8 shows the camera spectral response. Each blue point of the camera spectral response shown in Fig. 8 is obtained from polynomial interpolation of four red points

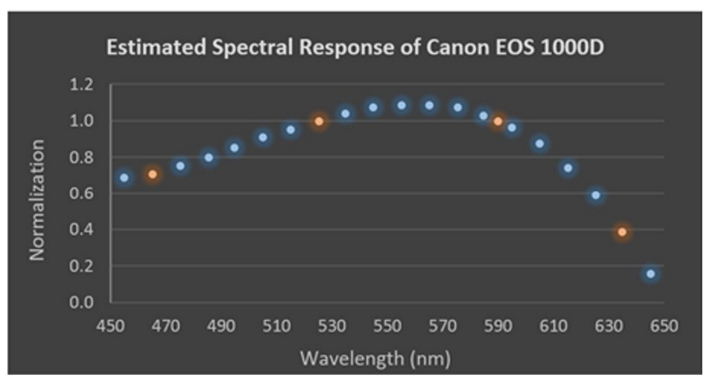

Fig. 8. Estimated spectral response of Canon EOS 1000D

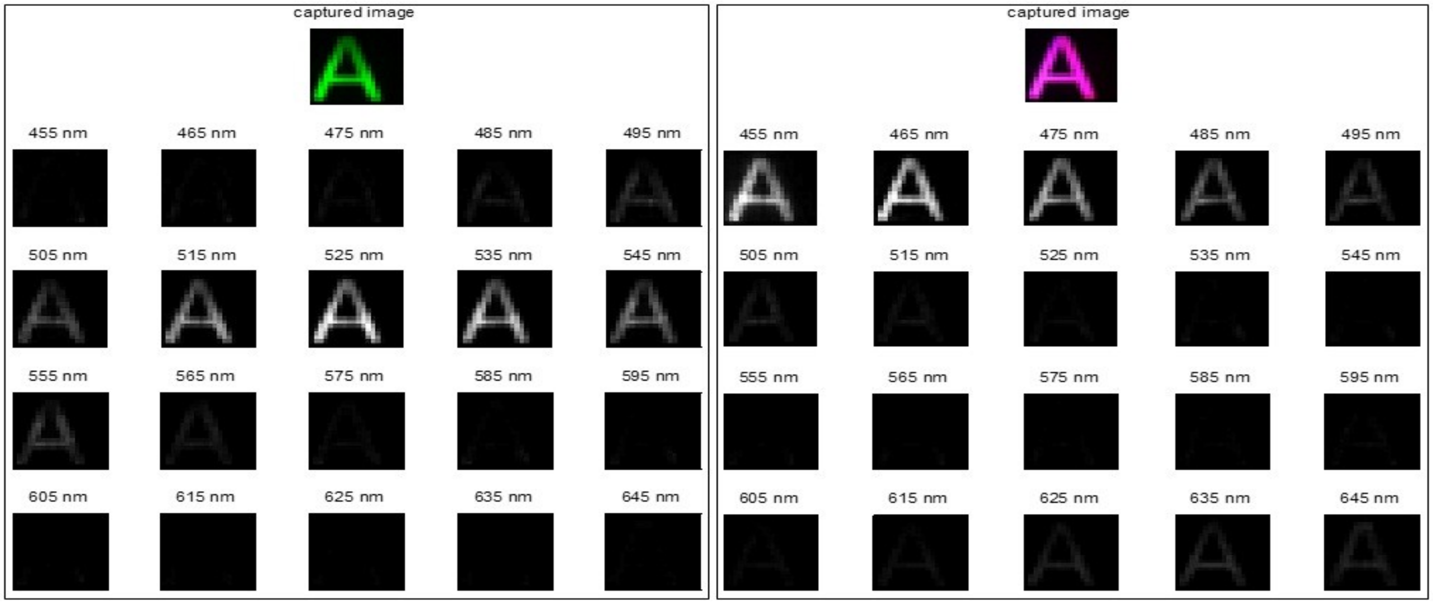

Fig. 9. The data cube of an object: at first condition of the experiment (left), and at second condition of the experiment (right).

V. RESULT AND DISCUSSIONS

The system uses a computer with 2GB RAM to run the reconstruction program. The result of the reconstruction program is a data cube in the form of 20 images that represents the intensity response of an object from 455 nm to 645 nm. The image of each band wavelength has a spatial size of 20×20 pixels.

An experiment needs to verify the capability of this system to reconstruct the right data cube. In this experiment, an object that is made by a white paper is placed in the spatial point plane as shown in Fig. 6. Then, the compact camera captures the object in two different conditions: while it is illuminated only by a 525 nm LED and while it is illuminated by 465 nm and 635 nm LEDs.

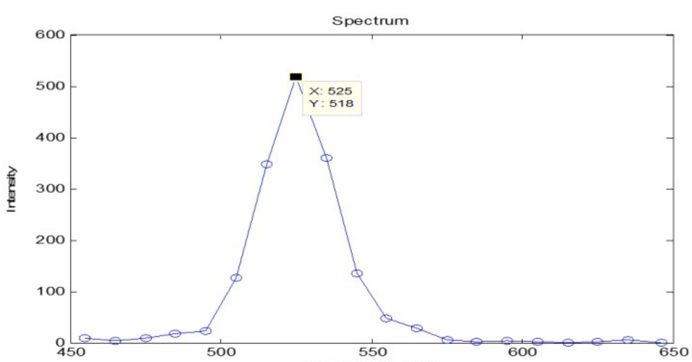

Fig. 10. Spectrum of a spatial coordinate on the data cube from the first experiment with 465 nm LED.

Fig. 10 shows the intensity response of a spatial coordinate on the data cube. The highest intensity of the spatial coordinate is located in wavelength of 525 nm. Fig. 9 (left) shows the result of the reconstruction program. It shows that the object in first condition of the experiment has a dominant intensity in 525 nm band of the data cube. The shape of the object also appears on the other measurement band, although with lower intensity.

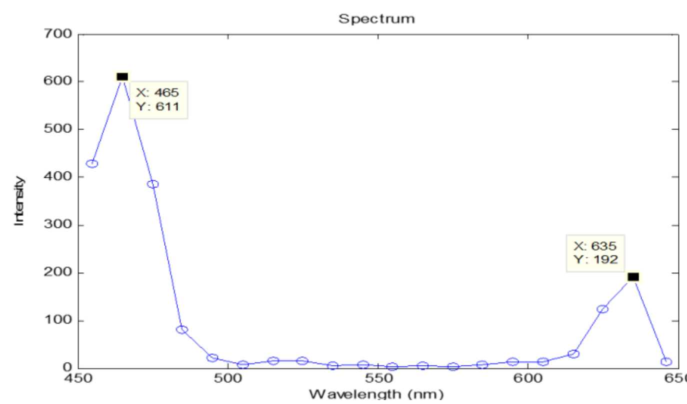

Fig. 11. Spectrum of a spatial coordinate on the data cube from the second experiment 465 and 635 nm LEDs.

Fig. 11 shows the intensity response of a spatial coordinate on the data cube. This spatial coordinate has spectrum with two peaks at wavelengths of 465 nm and 635 nm. The result of the reconstruction program at Fig. 9 (right) shows that the object in second condition of the experiment has a dominant intensity around 465 nm band and 635 nm band of the data cube. The experiment result shows the system's ability to generate a data cube with spatial and spectral information that is appropriate with the object conditions on the experiment. The system is also capable to measure spectrum from 455 nm to 645 nm.

VI. CONCLUSION

We have presented the design and implementation of a multispectral imaging system using a Canon EOS 1000D camera and CD elements as the diffraction device. The system can produce a data cube in form of 20 images that represent spatial intensity response of an object at 455 to 645 nm. The size of each reconstructed image is 20×20 pixels. The reconstruction program that employs EM algorithm is implemented using Matlab and run on a computer with 2 GB of RAM.

REFERENCES

[1] T. J. Cudahy, R. Hewson, J. F. Huntington, M. A. Quigley, P. S. Barry, "The performance of the satellite-borne Hyperion hyperspectral VNIR-SWIR imaging system for mineral mapping at Mount Fitton, South Australia," in *Int. Geosci. and Remote Sensing Symp*., Sydney, SY, 2001, pp. 314-416.

[2] A. O. N. Joseph, "Hyperspectral optical imaging for detection, diagnosis and staging of cancer," Ph.D. dissertation, Dept. Biomedical Eng., Univ. of Southern California, California, CA, 2012.

[3] N. J. Crane, E. G. Bartick, R. S. Perlman, S. Huffman, "Infrared spectroscopic imaging for noninvasive detection of latent fingerprints," *J. of Forensic Sci*., vol. 52, no. 1, pp. 48-53, 2007.

[4] D. Wu et al, "Application of time series hyperspectral imaging (TS-HSI) for determining water distribution within beef and spectral kinetic analysis during dehydration," *Food and Bioprocess Technology*, vol. 6, no. 11, pp. 2943-2958, 2013.

[5] A. F. H. Goetz, G. Vane, J. E. Solomon, and B. N. Rock, "Imaging spectrometry for earth remote sensing," *Sci*., vol. 228, no. 4704, pp. 1147-1153, 1985.

[6] G. Høye, and A. Fridman, "Mixel camera–a new push-broom camera concept for high spatial resolution keystone-free hyperspectral imaging," *Optics Express*, vol. 21, no. 9, pp. 11057-11077, 2013.

[7] J. Brauers, N. Schulte, and T. Aach, "Multispectral filter-wheel cameras: Geometric distortion model and compensation algorithms," *IEEE Trans. on Image Process*., vol. 17, no. 12, pp. 2368-2380, Dec. 2008.

[8] J. Y. Hardeberg, F. Schmitt, and H. Brettel, "Multispectral color image capture using a liquid crystal tunable filter," *Optical Eng*., vol. 41, no.10, pp. 2532–2548, 2002.

[9] R. Habel, M. Kudenov, and M. Wimmer, "Practical spectral photography," *Comput. Graph. Forum*, vol. 31, pp. 449-458. 2012.

[10] W. Lee, P. Lin, and C. Tseng, "The CD lens for optical engineering," *Int. J. of Eng. Educ*., vol. 22, no. 2, pp. 876-881, 2006.

[11] Thorlabs.com. (2016, August 1) PDA100A responsivity curve [online]. Available:https://www.thorlabs.com/newgrouppage9.cfm?objectgroup_id =3257&pn=PDA100A